Ionics (2008) 14:157–161
DOI 10.1007/s11581-007-0164-1

ORIGINAL PAPER

Lithium insertion studies on boron-doped diamond as a possible anode material for lithium batteries

A. Y. M. T. Christy · Kee Suk Nahm · Yun Ju Hwang · E. K. Suh · M. Anbu Kulandainathan · T. Premkumar · A. Manuel Stephan

Received: 28 September 2007 / Accepted: 28 September 2007 / Published online: 29 October 2007

Abstract Boron-doped diamond (BDD) was prepared by the hot filament chemical vapor deposition method. The prepared samples were subjected to X-ray diffraction, scanning electron microscopy, and Raman spectroscopy studies. The BDD composite electrode/Li cell has been assembled, and its cycling behavior was studied. The BDD possesses large sp^2 sites, which effectively participate in the lithium storage process. Furthermore, nanocrystalline tin (Sn) particles were prepared by the chemical reduction method. The addition of nanotin with the BDD-active material greatly enhances the cyclability of the cell.

Keywords Boron-doped diamond · XRD · Lithium batteries · Discharge capacity

Introduction

Although the lithium anode has superior theoretical capacity (3,800 mAh g^{-1}) and a high redox potential, there are several problems like dendrite and poor cyclability to be resolved before it can have practical applications [1–4]. For more than two decades, numerous researchers have endeavored to find solutions to this problem by introducing different solvent mixtures [5, 6], novel electrolyte salts [7], and additives to the electrolytes [8, 9]. Tin-based materials have been focused because of their high theoretical capacity (approximately three times higher than that of graphite, 994 mAh g^{-1}, the theoretical limit of Li4.4Sn). However, the large irreversible capacity caused by the reduction of the tin oxides and the formation of lithium oxide during the first cycle remain as an unsolved problem.

Indeed, large research efforts have been made in the development of lithium metal alloys (LiM) that possess a very high specific capacity and are expected to replace the conventional graphite in advanced lithium-ion high-energy batteries. As a promising approach, this M1M2 intermetallics, where the electrochemical process in a lithium cell involves the displacement of one metal, e.g., M2, which forms the desired lithium alloy, LiM2, while the other metal, M1 acts as an electrochemically inactive matrix to buffer the volume changes during the alloying process. However, these materials suffer from morphological changes during the charge–discharge cycling, which in turn results a very poor cycle life.

Recently, the doped diamond electrodes have drawn the attention of many researchers because of its appealing properties like small background current and good response to redox systems [10, 11]. This carbon electrode has the property of wide potential window in aqueous, nonaqueous, and ionic liquids, and it has the property of being chemically inert and stable in all kinds of solutions. Also of importance is that the boron-doped diamond (BDD) is hydrogen terminated, which in turn makes it a very stable surface and exhibits excellent electrochemical property than the other carbon forms like glassy carbon and highly oriented pyrolytic graphite. Lithium insertion into BDD is also of great interest in the recent years as this n-type semiconductor arises because of the high band gap of diamond.

In the present study, BDD was prepared by the chemical vapor deposition method, and its cycling performance was

A. Y. M. T. Christy · K. S. Nahm · Y. J. Hwang · E. K. Suh (✉)
School of Semiconductor and Chemical Engineering,
Chonbuk National University,
Chonju 561- 756, South Korea
e-mail: eksuh@chonbuk.ac.kr

M. A. Kulandainathan · T. Premkumar · A. M. Stephan
Central Electrochemical Research Institute,
Karaikudi 630 006, India

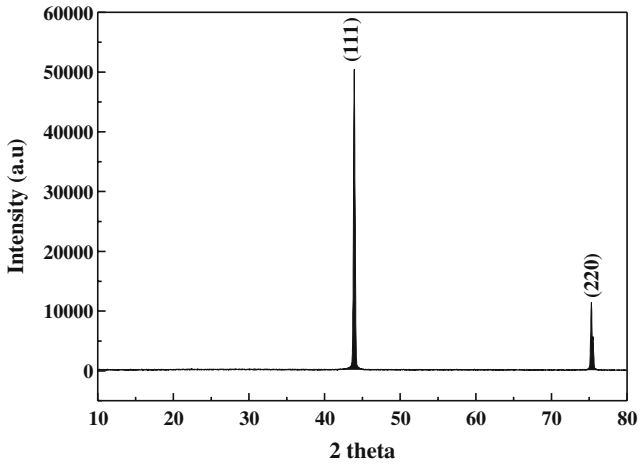

Fig. 1 X- ray diffractogram of boron-doped diamond

analyzed by assembling Li/BDD cells at ambient temperature. Furthermore, nanotin was added as an additive, and the cycling profile was examined.

Experimental procedure

Chemical reagents such as KCl and $Ru(NH_3)_6Cl_3$ were obtained from Aldrich and used without further purification. The demineralized and filtered water with a resistivity of not less than 18 MΩ were used in the preparation process. Both argon and hydrogen gases were used with a purity of 99.99%. BDD powders were prepared by using methanol, hydrogen, and diboron by the hot filament chemical vapor deposition (HF-CVD) on single crystal p-type Si (100) wafers. The doping level of boron expressed as B/C ratio was about 3,500 ppm. The obtained diamond film thickness was about 10 μm with a resistivity in the range of 10/30 ppm. This as grown BDD contains some graphitic (sp^2) phase and is hydrogen terminated. Activation of BDD by anodic polarization (in 1 M H_2SO_4 at 25 °C for 30 min) eliminates most of the sp^2 and absorbed hydrogen from the surface and is necessary to obtain reproducible electrochemical measurements.

Powder X-ray diffraction (XRD) patterns were recorded between 10 and 80° on a X-ray diffractometer, model (Rigaku D/Max 2500) fitted with a nickel-filtered CuK-α radiation source. The morphologies of the BDD was examined by a (FESEM S-4700, Hitachi) scanning electron microscope. Composite BDD electrodes for electrochemical lithium insertion studies were prepared by blade coating a slurry of 90 wt% of the pyrolytic carbon, 8 wt% of poly (vinylidene fluoride), and 2 wt% carbon black/nanotin of dispersed in *N*-methyl-2-pyrrolydone on a copper foil, followed by drying at 110 °C in an air oven, roller pressing the dried sheets, and punching out circular sheets. The composite BDD electrodes were coupled with lithium (Cyprus Foote Minerals) with an electrolyte of 1 M LiPF6 in a 1:1 (v/v) mixture of EC-DMC in 2,032 coin cells in an argon-filled glove box (OMNI-LAB system). The excess

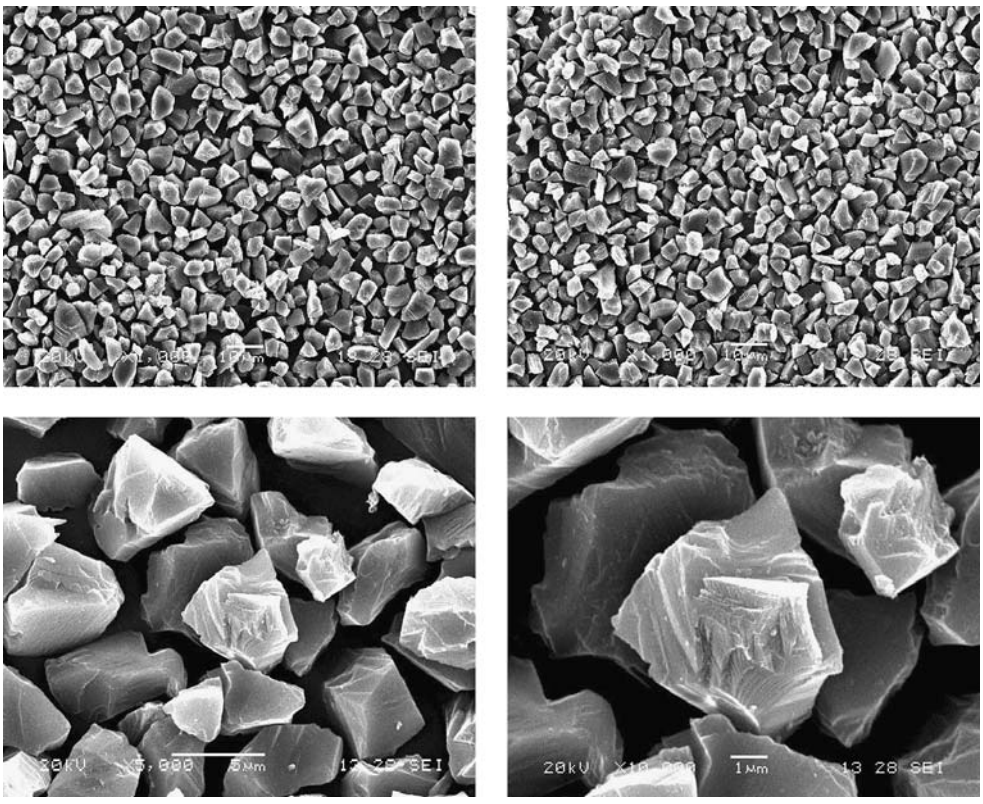

Fig. 2 SEM images of boron-doped diamond

lithium foil cut to size was employed as an anode, and composite BDD/BDD-Sn electrodes were employed as anode and cathode, respectively. Galvanostatic charge–discharge profiles were made between 3.000 and 0.002 V on a computer-controlled battery-testing unit (BTS 2004, Japan).

Results and discussion

The XRD pattern of BDD is displayed in Fig. 1. Two well-separated peaks around 2θ=43 and 75°, respectively, corresponds to faces of (111) and (220). These diffraction peaks are indexable to the Fd3m space group and are found to be face-centered cubic. The nit cell parameter was calculated as 9.3559 Å. These results are in accordance with Joint Committee on Powder Diffraction Standards data. Scanning electron microscopy (SEM) images of BDD are depicted in Fig. 2. The grains are faceted and are all more or less equally sized with an average size of 5 μm with a uniform texture that show a surface morphology with predominant (111) orientation (as shown in XRD as 100%).

The Raman spectrum of BDD is shown in Fig. 3. It is seen from the figure that the peak intensity observed at 1,332 cm^{-1} corresponds to the transversal mode, which is related to the sp^3 bond. The peak at 1,332 cm^{-1} and the peak that arises (not significant in the figure) approximately at 1,220 cm^{-1} are attributed to the relaxation of the Δk=0 selection rule caused by the small coherence length of the diamond crystallites [10–14].

Figure 4 shows the differential capacity vs potential for the Li/BDD cell between the voltage regions 0.002–3.0 V. Generally, lithium storage becomes more effective with increasing conductivity and also influenced by the grain size of the material [12]. Furthermore, the conductivity increases linearly with the increase of boron content in the diamond and in turn enhances the sp^2 sites. The sp^2 sites

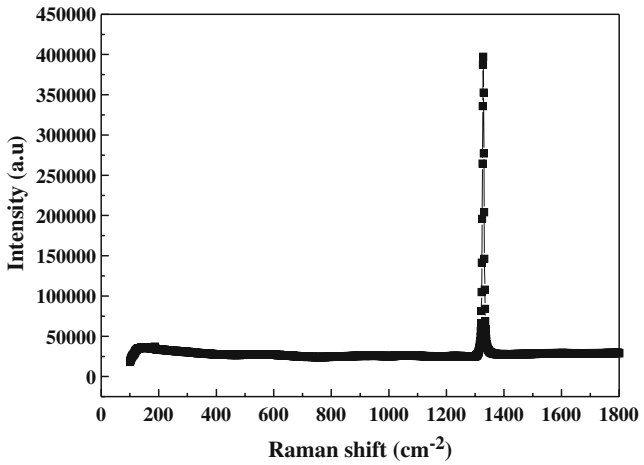

Fig. 3 Raman spectrum of boron-doped diamond

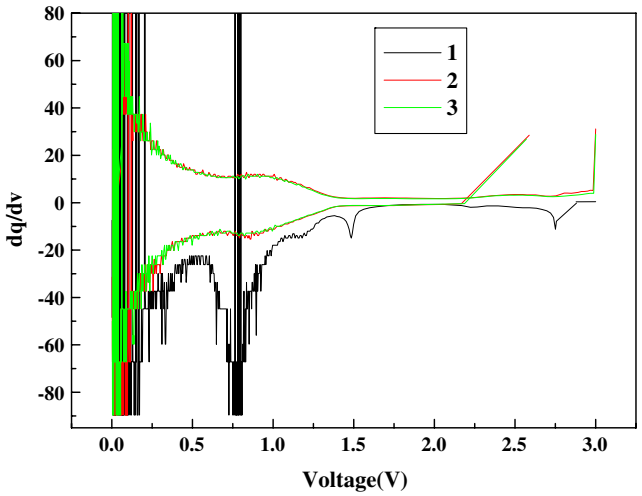

Fig. 4 Differential capacity (dQ/dT) vs potential of the Li/BDD cell. Cutoff voltage 0.002–3.0 V

that appear on the boundary of diamond grains and the sp^3 sites that present in the bulk of the diamond grains increases the lithium storage of the material. It is seen from the figure that two intense anodic and cathodic peaks appear, which, respectively, corresponds to the lithium insertion and extraction processes. In addition to that, a less intense peak is observed and is attributed to the decomposition of the electrolyte [12]. The chemical potential of electrons (Fermi level) and lithium-intercalated ions generally depend on the electronic and structural properties of the diamond materials. The sp^3 sites are active for lithium storage because the electrochemical intercalation of lithium can also occur even in insulating materials such as olivine [15–17]. When the electrons reach the grains, lithium intercalation is also possible even in insulators. In the present study, diamond grains of the BDD layer have effective participation in the lithium storage, and electron reaches the diamond through the sp^2 boundary, which is independent of diamond conductivity. Both graphitic and nongraphitic carbons provide sites for lithium insertion. Graphitic sp^2-type carbons accommodate Li between grapheme layers while the sp^3-type carbons can accommodate only in defect sites caused by the presence of the trivalent boron. The defect structure and, therefore, the sp^2 character can be enhanced by incorporation of more boron in the carbons.

Because no discernible line is observed less than 100 mV, it can be concluded that no metallic lithium deposition occurs on the BDD surface [12], and the cathodic and anodic charges are similar even in the third cycle, which shows that this system is reversible.

Figure 5a,b shows the cycling profile of BDD/Li cells with carbon black and nanotin as an additive, respectively. Figure 6a,b, respectively, shows the discharge capacity as a function of cycle number for the composite BDD/Li cells

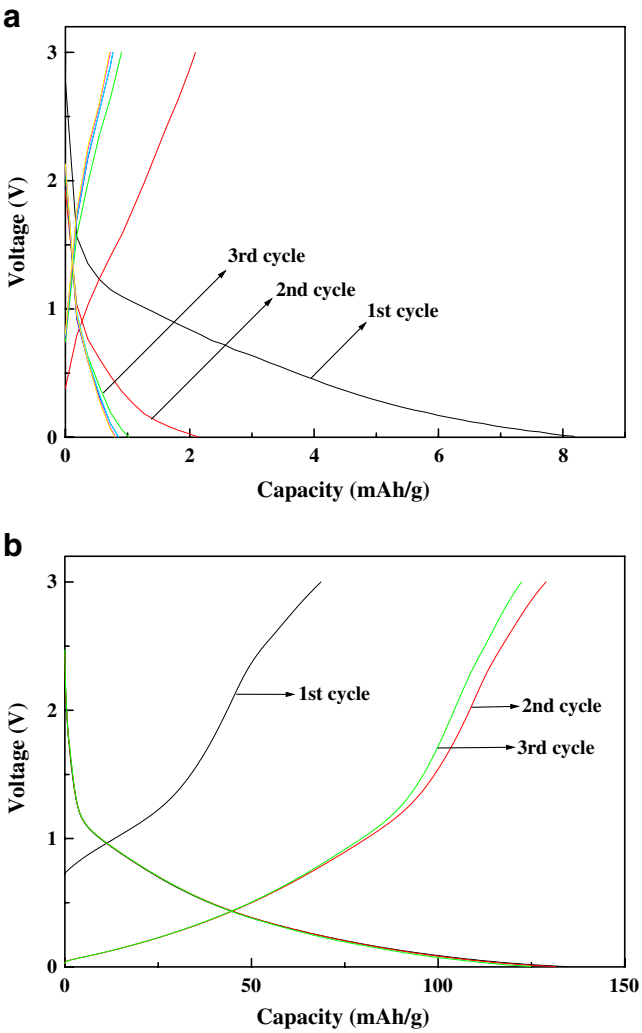

Fig. 5 **a** Cycling behavior of BDD/Li cells with carbon black as an additive. **b** Cycling behavior of BDD/Li cells with nanotin as an additive

comprising carbon black and nanotin (as an additive during electrode preparation) as described in "Experimental procedure." The addition of nanotin with the active material has considerably enhanced the discharge capacity of the cell. Also of importance is that a stable cycling behavior is seen even after ten cycles. A similar study was observed by Wang et al. [18], where the authors reported the formation of LiSn alloys. According to the authors, lithium reacts with Sn and forms a Li_xSn alloy in a nanocrystalline or amorphous state. In addition, Sn many be isolated because of the cracking in the subsequent cycles and may increase the impedance of the cell. Lee et al. [19] and Hwang et al. [20] observed an enhanced cycling stability upon the addition of nanotin, respectively, for the synthetic graphite and coconut carbonaceous materials. Complete lithiation of tin and delithiation of the resulting $Li_{22}Sn_5$ alloy are accompanied by volume changes of as much as 259%, which limits the applicability of Sn as a lithium-insertion anode. One of the ways to circumvent this problem is to use composites in which the second phase helps buffer strains because of volume changes. In our case, the BDD particles by virtue of this intergranular space available between them provides the necessary resistance during charge–discharge. A comparison of Fig 6a,b shows that the first cycle deliverable capacities of the BDD and Sn-BDD samples were about 10 and 130 mAh g^{-1}, respectively. Considering that the share in the capacity from nanotin cannot exceed the theoretical values of 20 mAh g^{-1} for a composite with 2% Sn, a jump in the capacity of the composite by more than 100 mAh g^{-1} looks extraordinary. Further, studies are required to unravel this behavior.

The electrochemical properties of the various content of boron doped in the diamond and determination of the ratio of sp^3/sp^2 by X-ray photoelectron spectroscopy analysis are underway. The mechanism for the enhanced stability upon

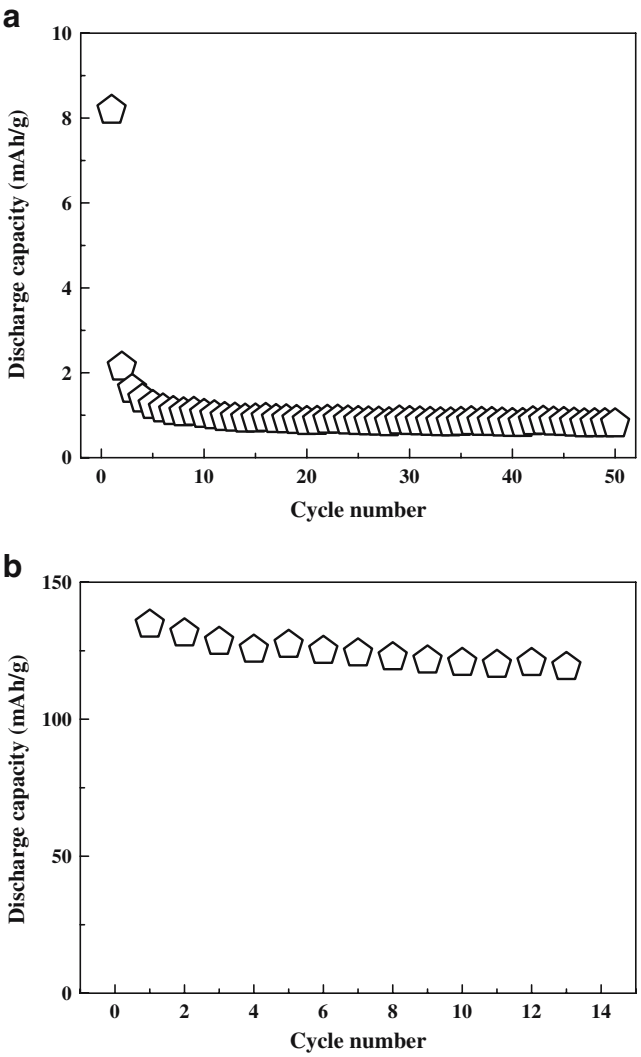

Fig. 6 **a** Discharge capacity vs cycle number of Li/composite BDD cell with carbon black as an additive. **b** Discharge capacity vs cycle number of Li/composite BDD cell with nanotin as an additive

the addition of nanotin is also being studied and will be communicated in the upcoming report. It is to be noted that although a reversible capacity of 125 mAh g^{-1} appears low as compared to more than 300 mAh g^{-1} for graphites, it is comparable with 130–140 mAh g^{-1} that cathodes such as $LiCoO_2$ can offer.

Conclusions

BDD was prepared by the HF-CVD method and was subjected to XRD, SEM, Raman, and charge–discharge studies. The results suggest that BDD anode materials will be very promising if BDD provides an elevated number of sp^2 and sp^3 sites with good intercalation kinetics.

Acknowledgments This work was supported by the Korean Research Foundation Grant funded by the Korean Government (MOEHRD; KRF-2005-005-J07501). One of the authors M.A.K. gratefully acknowledges Prof. Frank Marken, University of Bath, UK, and Prof. Clive Hall, Washway Consultants, The Netherlands, for the discussion on the boron-doped diamond.

References

1. Zhang JJ, Xia YY (2006) J Electrochem Soc 153:A1466
2. Tamura N, Kato Y, Mikami A, Kamino M, Matsuta S, Fujitani S (2006) J Electrochem Soc 153:A1626
3. Hassoun J, Panero S, Scrosati B (2006) JPower Sources 160:1336
4. Jusef H, Panero S, Simon P, Taberna PL, Scrosati B (2007) Adv Mater 38:1632
5. Hirai T, Yoshimatsu I, Yamaki JI (1994) J Electrochem Soc 141:611
6. Wang X, Yasukawa E, Kasuya S (2001) Electrochim Acta 46:813
7. Ishikawa M, Machine SI, Morita M (1999) J Electroanal Chem 473:279
8. Kanamura K, Takezawa H, Shiraishi S, Takehara Z (1994) J Electrochem Soc 144:1990
9. Mogi R, Inaba M, Jeong SK, Iriyama Y, Abe T, Ogumi Z (2002) J Electrochem Soc 149:A1578
10. Ferreira NG, Silva LLG, Carot EJ (2002) Diamond Relat Mater 11:657
11. Ferreira NG, Silva LLG, Carot EJ (2002) Diamond Relat Mater 11:1523
12. Zhang RJ, Lee ST, Lam YM (1996) Diamond Relat Mater 5:1288
13. Nemanich RJ, Glass JT, Lukovsky G, Shroder RE, Vac J (1988) Sci Technol A6:1783
14. Clement CL, Zenia F, Ndao NA, Deneuville A (1999) New Diam Front Carbon Technol 19:189
15. Almeida EC, TRava- Airoldi VJ, Ferreira NG, Rosolen JM (2005) Diamond Related Mater 14:1673
16. Airoldi VJT, Ferreira NG, Mendonca LL, Rosolen JM (2003) Diamond Related Mater 12:596
17. Girard HA, Simon N, Ballutard D, de La Rochefoucauld E (2007) A Etcheberry Diamond Related Mater 16:888
18. Wang GX, Ahn JH, Lindsay MJ, Sun L, Bradhurst DH, Dou SX, Liu HK (2001) J Power Sources 97–98:211
19. Lee JY, Zhang R, Liu Z (2000) J Power Sources 90:75
20. Hwang YJ, Jeong SK, Shin JS, Nahm KS Manuel Stephan A (2007) J Alloys Compd (in press) available online November 9, 2007